Deficiency of autotaxin/lysophospholipase D results in head cavity formation in mouse embryos through the LPA receptor-Rho-ROCK pathway

doi: 10.1016/j.bbrc.2010.08.008

Deficiency of autotaxin/lysophospholipase D results in head cavity formation in mouse embryos through the LPA receptor-Rho-ROCK pathway

Seiichi Koike[a, b], Kazuko Keino-Masu[a], Masayuki Masu[a]

[a] Department of Molecular Neurobiology, Graduate School of Comprehensive Human Sciences, University of Tsukuba, 1-1-1 Tennodai, Tsukuba, Ibaraki 305-8577, Japan

[b] Present address: Department of Neurobiology, Max Planck Institute of Biophysical Chemistry, Am Faßberg 11, 37077 Göttingen, Germany

Correspondence should be addressed to Masayuki Masu, Department of Molecular Neurobiology, Graduate School of Comprehensive Human Sciences, Institute of Basic Medical Sciences, University of Tsukuba, 1-1-1 Tennodai, Tsukuba, Ibaraki 305-8577, Japan

Phone: +81-29-853-3249

Fax: +81-29-853-3498

E-mail: mmasu@md.tsukuba.ac.jp

Abbreviations: DIV, day *in vitro*; E, embryonic day; ENPP2, ectonucleotide pyrophosphatase/phosphodiesterase 2; LPA, lysophosphatidic acid; MAPK, mitogen activated protein kinase; PI3K, phosphatidylinositol 3-kinase: PLC, phospholipase C: ROCK, Rho-associated coiled-coil containing protein kinase; S1P, sphingosine 1-phosphate; VE, visceral endoderm.

Abstract

Autotaxin, encoded by the *Enpp2* gene, generates lysophosphatidic acid (LPA) extracellularly, eliciting various cellular responses through specific LPA receptors. Previous studies have revealed that *Enpp2*$^{-/-}$ mice die at E9.5 owing to angiogenic defects in the yolk sac. Moreover, *Enpp2*$^{-/-}$ embryos show growth retardation, allantois malformation, no axial turning, and head cavity formation. We have also demonstrated that lysosome biogenesis is impaired in yolk sac visceral endoderm cells of *Enpp2*$^{-/-}$ embryos as a result of the downregulation of the Rho-ROCK (Rho-associated coiled-coil containing protein kinase)-LIM kinase pathway. In this study, we examine what signaling defect(s) is responsible for head cavity formation and yolk sac angiogenic defects. By using a whole embryo culture system, we show that 10 μM Ki16425, an antagonist for the LPA receptors, induces head cavity formation and yolk sac angiogenic defects in wild-type embryos. Moreover, 1 μM Ki16425 induces both phenotypes in *Enpp2* heterozygous embryos at significantly higher incidence than in wild-type embryos, suggesting an interaction between autotaxin and LPA receptor signaling. Furthermore, we show that inhibition of the Rho-ROCK pathway induces head cavity formation, whereas multiple pathways are involved in yolk sac angiogenic defects. These results reveal the signal transduction defects that underlie the abnormalities in *Enpp2*$^{-/-}$ embryos.

Keywords: autotaxin; LPA; Enpp2; Rho; ROCK; knockout mouse

Introduction

Autotaxin, also known as ENPP2 (ectonucleotide pyrophosphatase/phosphodiesterase 2), is an exoenzyme having lysophospholipase D activity that generates lysophosphatidic acid (LPA) in the extracellular space [1, 2]. It elicits a wide variety of biological responses such as cell proliferation, migration, survival, and neurite retraction through activating specific G protein-coupled receptors (LPA_{1-6}) [3-7]. LPA receptors are coupled to several intracellular pathways, including Rho/ROCK (Rho-associated coiled-coil containing protein kinase), phosphatidylinositol 3-kinase (PI3K), mitogen activated protein kinase (MAPK), and phospholipase C (PLC) pathways through distinct G proteins [3-7]. In addition to LPA production, autotaxin was shown to generate sphingosine 1-phosphate (S1P) *in vitro* [8] although the *in vivo* roles of autotaxin in S1P production remain to be established.

Several studies have shown that *Enpp2*$^{-/-}$ mice die at E9.5 owing to angiogenic defects in the yolk sac [9-13]. *Enpp2*$^{-/-}$ embryos also show pleiotropic defects, such as growth retardation, allantois malformation, neural tube defects, no axial turning, and head cavity formation [9-13]. In addition, adult *Enpp2*-heterozygous mice show half-normal levels of lysophospholipase D activity and LPA, but normal levels of S1P, in plasma [9, 10], suggesting that autotaxin is a major LPA-producing enzyme *in vivo*.

In a previous study, we demonstrated that lysosome biogenesis was impaired in yolk sac visceral endoderm (VE) cells of *Enpp2*$^{-/-}$ embryos [12]. By using a whole embryo culture system combined with specific inhibitors, we showed that the control of actin turnover dynamics through the Rho-ROCK-LIM kinase pathway was required to form large lysosomes in VE cells [12]. However, it remains unknown what signaling defect(s) is responsible for other phenotypes of *Enpp2*$^{-/-}$ embryos.

Here, we show that inhibition of the LPA receptors induces head cavity formation and yolk sac angiogenic defects in a whole embryo culture. In addition, we show that blockade of the Rho/ROCK pathway results in the head cavity formation, whereas multiple pathways are involved in the angiogenic defects. These findings demonstrate the specific role of the LPA receptor-Rho-ROCK pathway in head cavity formation in *Enpp2*$^{-/-}$ embryos.

Materials and methods

Animal Experiments. All the experiments using animals were approved by the Animal Care and Use Committee of the University of Tsukuba and performed under its guidelines. Noon of the day on which a vaginal plug was observed was taken as embryonic day 0.5 (E0.5). *Enpp2*-deficient mice were generated and genotyped as described previously [12]. Timed-pregnant ICR mice (CLEA Japan, Tokyo, Japan; Japan SLC, Hamamatsu, Japan) were used for the pharmacological experiments.

Histology, immunohistochemistry, and LacZ staining. Embryos were fixed with 4% paraformaldehyde/PBS at 4°C overnight. For histological examination, 4-μm-thick paraffin sections were stained with hematoxylin and eosin. For PECAM-1 immunostaining, 10-μm-thick cryostat sections were treated with 0.3% H_2O_2 in PBS, blocked with PBS supplemented with 1% heat-inactivated normal goat serum and 0.1% Tween 20, and then incubated with anti-PECAM-1 (1:400; BD Biosciences Pharmingen, San Diego, CA, USA) at 4°C overnight. After washing, the slides were incubated with biotin-SP-conjugated anti-rat IgG (1:500; Jackson ImmunoResearch, West Grove, PA, USA), followed by the chromogenic staining using a VECTASTAIN Elite ABC kit and DAB substrate kit (Vector Laboratories, Burlingame, CA, USA). For SMA immunostaining, the slides were incubated with HRP-conjugated anti-SMA (DAKO, Glostrup, Denmark),

followed by fluorescent signal detection using a TSA kit #12 (Invitrogen, Carlsbad, CA, USA). LacZ staining was carried out by incubating the fixed embryos in PBS containing 5 mM $K_4Fe(CN)_6$, 5 mM $K_3Fe(CN)_6$, 1 mg/ml X-gal, 2 mM $MgCl_2$, 0.02% Nonidet P40, and 0.01% Na deoxycholate.

RT-PCR. Reverse transcription and PCR were performed as previously described [12]. Quantitative PCR was carried out using a LightCycler and LightCycler FastStart DNA Master SYBR Green I reagent (Roche Diagnostics, Basel, Switzerland). Expression levels were normalized by β-actin expression. Primer sequences and PCR conditions are available upon request.

Ex vivo whole embryo culture. Whole embryo culture was performed as previously described [12, 14]. Briefly, embryos were dissected at E7.5 and cultured in 100% rat serum (Charles River, Yokohama, Japan) supplemented with 2 mg/ml glucose in a culture bottle placed in a rotation drum culture system (Ikemoto Rika, Tokyo, Japan) at 37°C under 5% O_2, 5% CO_2 and 90% N_2 for the initial 24h, followed by 20% O_2, 5% CO_2 and 75% N_2 for the next 24 h. The reagents used were Ki16425 (1-10 μM; Sigma-Aldrich, St. Louis, MO, USA), VPC 23019 (1-10 μM; Avanti Polar Lipids, Alabaster, AL, USA), *Clostridiusm botulinum* exoenzyme C3 (20 μg/ml; Calbiochem, Darmstadt, Germany), H1152 (0.1 μM; Calbiochem), pertussis toxin (0.5 μg/ml; Calbiochem), LY294002 (10 μM; Sigma-Aldrich), PD98059 (10 μM; Calbiochem), U-73122 (10 μM; Sigma-Aldrich), and cytochalasin B (0.03-0.3 μM; Calbiochem).

Results

Enpp2$^{-/-}$ embryos have abnormal cavities in the head and trunk regions

We re-examined *Enpp2$^{-/-}$* embryos and found that abnormalities appeared at earlier stages than previously reported [9-13]; at E7.5, a small cavity had formed between the

embryonic endoderm and mesoderm (Figures 1A-B). At E8.5, a large cavity was found in the head mesenchyme in all *Enpp2*$^{-/-}$ embryos (Figures 1C-E) as reported previously [9-13]. At E9.5, most *Enpp2*$^{-/-}$ embryos showed arrested development (Figure 1F). The head cavities were confined to one side in most *Enpp2*$^{-/-}$ embryos from E7.5 to E8.5, whereas they were present bilaterally at E9.5. Some *Enpp2*$^{-/-}$ embryos had cavities in the trunk region at E9.5 (Figure 1G).

Enpp2$^{-/-}$ *embryos have angiogenic defects of the yolk sac*

Enpp2$^{-/-}$ embryos show angiogenic defects in the yolk sac [9-13]. In *Enpp2*$^{-/-}$ embryos, endothelial cells, stained with the endothelial cell marker PECAM-1/CD31, had formed a nearly normally honeycomb-like vascular plexus at E8.5 (Figures 1J, L, N), whereas branched vitelline vessels were not formed at E9.5 (Figure 1R, T, V). Thus, *de novo* differentiation of endothelial cells ("vasculogenesis" [15]) appeared to be normal, whereas maturation and remodeling of blood vessels ("angiogenesis" [15]) were impaired in *Enpp2*$^{-/-}$ embryos. Smooth muscle cells, revealed by smooth muscle actin immunostaining, appeared to form normally in *Enpp2*$^{-/-}$ embryos (Figure 1O-P, W-X).

We next examined the expression of cell-type specific markers for the yolk sac: vascular endothelial zinc finger (*Vezf1*), vascular endothelial growth factor receptor 2 (*Flk1*/*Kdr*), and endoglin (*Eng*) for endothelial cells; smooth muscle actin (*Acta2*) and SM22α (*Tagln*) for pericytes/smooth muscle cells; alpha fetoprotein (*Afp*), quaking (*Qk*), claudin7 (*Cldn7*), and hepatocyte nuclear factor 4α (*Hnf4a*) for VE cells. Semi-quantitative RT-PCR showed that expression of these markers was comparable between the control and *Enpp2*$^{-/-}$ embryos at E8.5 (Figure 1Y, data not shown). In addition, angiogenesis-promoting factors, such as vascular endothelial growth factor A (*Vegfa*), transforming growth factor β1 (TGFβ1; *Tgfb1*), and angiopoietin-1 (*Ang1*), were

expressed normally in *Enpp2*$^{-/-}$ yolk sacs and embryos proper at E8.5. In contrast, at E9.5, *Vegfa*, *Tgfb1*, and *Ang1* were upregulated in *Enpp2*$^{-/-}$ embryos proper (about 6.8-, 2.4-, and 1.8-fold, respectively, as assessed by quantitative PCR), suggesting that *Enpp2*$^{-/-}$ embryos became hypoxic because of vascular insufficiency (Figure 1Y). Furthermore, expression of an apoptosis-associated gene, *Gadd153*, was upregulated and many TUNEL-positive cells were detected in the E9.5 embryos proper (Figure 1Y, data not shown).

Taken together, these findings indicate that the head cavity was formed well before the deterioration of *Enpp2*$^{-/-}$ embryos, which started at about E9.5 when angiogenic defects were evident. Therefore, in the following experiments, we focused on two obvious and robust phenotypes at relatively healthy stages, head cavity formation at E8.5 and yolk sac angiogenic defects at E9.5, and examined the signal transduction defects responsible for these phenotypes.

A whole embryo culture system mimics in vivo development faithfully

To examine the downstream pathways of autotaxin, we used an *ex vivo* whole embryo culture [12, 16]. This is a well-established system that is useful for studying normal development and developmental toxicity *in vitro* [16]. When E7.5 wild-type embryos were cultured for 1 or 2 days, they showed a normal appearance comparable to those of *in-utero*-grown E8.5 and E9.5 embryos, respectively (Figure 2A, E, I). In addition, when blood vessels were visualized using whole-mount lacZ staining of the embryos carrying *E. coli lacZ* in the *Flk1* gene (*Flk1*^{lacZ} mice, a kind gift of J. Rossant) [17], normal branched vitelline vessels were observed in wild-type embryos after 2 days of culture (Figure 2M). In contrast, when *Enpp2*$^{-/-}$ embryos were cultured for 1 day, most of them had head cavities (Figures 2F, Q) that were indistinguishable from those of E8.5 *Enpp2*$^{-/-}$ embryos grown *in utero*. Moreover, all *Enpp2*$^{-/-}$ embryos showed yolk sac angiogenic

defects (Figures 2J, N, R) that were indistinguishable from those seen in the E9.5 *Enpp2*$^{-/-}$ embryos grown *in utero*. These results indicate that a whole embryo culture system mimics *in vivo* development of wild-type and *Enpp2*$^{-/-}$ embryos faithfully, thus making it suitable for testing whether blockade of the downstream signal transduction pathways induces the defects observed in *Enpp2*$^{-/-}$ embryos. In the following experiments, we used inhibitors at the concentrations determined in our previous study [12].

Blockade of LPA receptors leads to head cavity formation

We first tested inhibitors of LPA and S1P receptors. When wild-type mouse embryos were cultured with Ki16425, an LPA_1/LPA_3 antagonist [18], for 1 day, the head cavity was formed in a dose-dependent manner; 10 μM Ki16425 induced the cavity formation to the same extent as that observed in non-treated *Enpp2*$^{-/-}$ embryos. (Figure 2G, Q). In contrast, 10 μM VPC23019, an $S1P_1/S1P_3$ antagonist [19], did not induce head cavity formation (Figure 2H, Q). These findings indicate that LPA receptors are the major mediators downstream of autotaxin.

We further examined the functional linkages between autotaxin and LPA receptors in another way. Because *Enpp2* heterozygous mice show half-normal levels of LPA [9, 10], thus having reduced levels of downstream signaling, they should be more sensitive to the inhibitors than are wild-type mice. We thus tested whether a subthreshold level of the inhibitors can induce abnormalities in the heterozygous mice. When *Enpp2*$^{+/+}$ embryos were cultured with 1 μM of Ki16425, head cavity formation was induced at low incidence (n = 2/17), whereas the same concentration of Ki16425 induced head cavity formation at significantly higher incidence (n = 12/23) in *Enpp2*$^{+/-}$ embryos ($P < 0.01$, chi-square test for independence) (Figure 2S), suggesting an interaction between autotaxin and LPA receptor signaling. In contrast, treatment with 1 μM VPC23019 led to a slight increase of

head cavity formation in *Enpp2*$^{+/-}$ embryos (n = 3/14) compared with *Enpp2*$^{+/+}$ embryos (n = 0/10), but the difference was not significant ($P > 0.05$) (Figure 2S). These findings demonstrate that the defects in LPA receptors, but not in S1P receptors, underlie head cavity formation in *Enpp2*$^{-/-}$ embryos.

Blockade of LPA receptors leads to yolk sac angiogenic defects

In contrast to head cavity formation, either 10 μM Ki16425 or 10 μM VPC23019 induced yolk sac angiogenic defects (Figure 2O-P, R), suggesting that both LPA and S1P receptors are required for normal angiogenesis. These findings are compatible with those of previous reports that autotaxin promotes angiogenesis in cultured endothelial cells or in a murine *in vivo* angiogenesis model [20] and that both LPA and S1P have angiogenic activity *in vitro* and *in vivo* [21-23].

We wondered whether both pathways function downstream of autotaxin. To address this question, we again tested whether *Enpp2* heterozygous mice were more sensitive to the inhibitors. A low concentration (1 μM) of Ki16425 induced a significantly higher incidence of angiogenic defects in *Enpp2*$^{+/-}$ embryos than in *Enpp2*$^{+/+}$ embryos (*Enpp2*$^{+/+}$, n = 1/8; *Enpp2*$^{+/-}$, n = 5/8; $P < 0.01$, chi-square test for independence) (Figure 2T), suggesting an interaction between autotaxin and LPA receptors in angiogenesis. In contrast, treatment with 1 μM VPC23019 resulted in a slight increase of angiogenic defects in *Enpp2*$^{+/-}$ embryos (n = 5/12) compared with those in *Enpp2*$^{+/+}$ embryos (n = 1/6), but the difference was not significant ($P > 0.05$) (Figure 2T). These data suggest that S1P receptors have little, if any, significance in autotaxin-mediated angiogenesis in the yolk sac. Taken together, these findings indicate that the defects in LPA receptor signaling are responsible for head cavity formation and yolk sac angiogenic defects in *Enpp2*$^{-/-}$ embryos.

Blockade of the Rho/ROCK signaling pathway leads to head cavity formation

The major downstream pathways of LPA receptors are $G_{12/13}$-RhoA, G_i-PI3K-Rac, G_i-MAPK, and G_q-PLC [3-7]. We thus examined which signaling pathway(s) is associated with the phenotypes of *Enpp2*$^{-/-}$ embryos. Treatment of embryos with a Rho inhibitor, *Clostridium* C3 exoenzyme (20 μg/ml), or a ROCK inhibitor, H1152 (0.1 μM), resulted in head cavity formation, whereas treatment with a G_i inhibitor, pertussis toxin (0.5 μg/ml); a PI3K inhibitor, LY294002 (10 μM); a MAPK inhibitor, PD98059 (10 μM); or a PLC inhibitor, U-73122 (10 μM), showed no significant effects on head cavity formation (Figure 3A-F, S). These findings suggest that the Rho/ROCK pathway is specifically involved in head cavity formation.

Blockade of multiple signaling pathways leads to yolk sac angiogenic defects

In contrast to head cavity formation, all the inhibitors used in this study (C3 exoenzyme, H1152, pertussis toxin, LY294002, PD98059, and U-73122) induced angiogenic defects (Figure 3M-R, T). These findings indicate that Rho, ROCK, G_i, PI3K, MAPK, and PLC are required for some aspects of angiogenesis in the yolk sac.

Blockade of actin polymerization leads to head cavity and yolk sac angiogenic defects

Because LPA induces Rho-mediated cytoskeletal rearrangement, we wondered whether direct perturbation of the actin cytoskeleton caused the abnormalities observed in *Enpp2*$^{-/-}$ embryos. We addressed this question by treating mouse embryos with cytochalasin B, a cell-permeable inhibitor of actin polymerization. When mouse embryos were cultured with cytochalasin B, it induced head cavity formation and angiogenic defects in a dose-dependent manner (Figure 4). This result suggests that actin depolymerization leads to head cavity formation and angiogenesis in the yolk sac.

Discussion

In this study, we showed that blockade of LPA receptors led to head cavity formation and angiogenic defects in mouse embryos. Moreover, we demonstrated that the Rho-ROCK pathway was specifically associated with the head cavity formation, whereas multiple intracellular signaling pathways were involved in angiogenesis. These latter results are compatible with the findings of previous reports that gene disruption of the components of G_{12} (*Gna12*)/G_{13} (*Gna13*), MAPK (*Mekk3*), PLC (*Plcg1*), or PI3K (*Pik3ca*) led to angiogenic defects in the yolk sac [24-28].

Head cavity formation is a very characteristic phenotype in *Enpp2*$^{-/-}$ embryos. To the best of our knowledge, there has been no report of knockout mice that have cavities in the head mesenchyme, while only a teratogen, trypan blue, was reported to induce similar head cavities in rat embryos *in vitro* and *in vivo* [29]. Trypan blue inhibited lysosome functions in yolk sac VE cells [30], which play a critical role in the maternofetal exchange of nutrients prior to the formation of the chorioallantoic placenta [31, 32]. In addition, a previous study suggested that osmotic imbalance as a result of the transport defects of VE cells resulted in head cavity formation [29]. When cavities were formed in *Enpp2*$^{-/-}$ embryos, the cells surrounding the cavities appeared to be deformed as if squeezed by pressure, suggesting that the cavity was formed as the result of abnormal fluid accumulation. Given that *Enpp2*$^{-/-}$ embryos have lysosomal defects in VE cells [12], and that the inhibitors of the Rho-ROCK pathway specifically lead to the defects in lysosome biogenesis [12] and head cavity formation (this study), osmotic imbalance caused by the VE cell dysfunction may induce head cavity formation in *Enpp2*$^{-/-}$embryos. Further studies are necessary to elucidate the link between cavity formation and abnormalities in VE cells.

Acknowledgements

We thank J. Rossant and M. Ema for *Flk1*^{lacZ} mice; N. Osumi for the protocol of whole embryo culture; and F. Miyamasu for useful comments on the manuscript. This work was partly supported by Grants-in-Aid for Scientific Research on Priority Areas and the 21st Century COE program from the Ministry of Education, Culture, Sports, Science, and Technology of Japan.

References

[1] A. Tokumura, E. Majima, Y. Kariya, K. Tominaga, K. Kogure, K. Yasuda, K. Fukuzawa, Identification of human plasma lysophospholipase D, a lysophosphatidic acid-producing enzyme, as autotaxin, a multifunctional phosphodiesterase, J. Biol. Chem. 277 (2002) 39436-39442.

[2] M. Umezu-Goto, Y. Kishi, A. Taira, K. et al., Autotaxin has lysophospholipase D activity leading to tumor cell growth and motility by lysophosphatidic acid production, J. Cell Biol. 158 (2002) 227-233.

[3] B. Anliker, J. Chun, Cell surface receptors in lysophospholipid signaling, Semin. Cell Dev. Biol. 15 (2004) 457-465.

[4] C. Stefan, S. Jansen, M. Bollen, NPP-type ectophosphodiesterases: unity in diversity, Trends Biochem. Sci. 30 (2005) 542-550.

[5] D. Meyer zu Heringdorf, K.H. Jakobs, Lysophospholipid receptors: signalling, pharmacology and regulation by lysophospholipid metabolism, Biochim. Biophys. Acta 1768 (2007) 923-940.

[6] L.A. van Meeteren, W.H. Moolenaar, Regulation and biological activities of the autotaxin-LPA axis, Prog. Lipid Res. 46 (2007) 145-160.

[7] K. Noguchi, D. Herr, T. Mutoh, J. Chun, Lysophosphatidic acid (LPA) and its receptors, Curr. Opin. Pharmacol. 9 (2009) 15-23.

[8] T. Clair, J. Aoki, E. Koh, et al., Autotaxin hydrolyzes sphingosylphosphorylcholine to produce the regulator of migration, sphingosine-1-phosphate, Cancer Res. 63 (2003) 5446-5453.

[9] M. Tanaka, S. Okudaira, Y. Kishi, et al., Autotaxin stabilizes blood vessels and is required for embryonic vasculature by producing lysophosphatidic acid, J. Biol. Chem. 281 (2006) 25822-25830.

[10] L.A. van Meeteren, P. Ruurs, C. Stortelers, et al., Autotaxin, a secreted lysophospholipase D, is essential for blood vessel formation during development, Mol. Cell. Biol. 26 (2006) 5015-5022.

[11] G. Ferry, A. Giganti, F. Coge, F. Bertaux, K. Thiam, J.A. Boutin, Functional invalidation of the autotaxin gene by a single amino acid mutation in mouse is lethal, FEBS Lett. 581 (2007) 3572-3578.

[12] S. Koike, K. Keino-Masu, T. Ohto, F. Sugiyama, S. Takahashi, M. Masu, Autotaxin/lysophospholipase D-mediated lysophosphatidic acid signaling is required to form distinctive large lysosomes in the visceral endoderm cells of the mouse yolk sac, J. Biol. Chem. 284 (2009) 33561-33570.

[13] S. Fotopoulou, N. Oikonomou, E. Grigorieva, et al., ATX expression and LPA signalling are vital for the development of the nervous system, Dev. Biol. 339 (2010) 451-464.

[14] N. Osumi-Yamashita, Y. Ninomiya, K. Eto, Mammalian craniofacial embryology in vitro, Int. J. Dev. Biol. 41 (1997) 187-194.

[15] W. Risau, Mechanisms of angiogenesis, Nature 386 (1997) 671-674.

[16] P.P. Tam, Postimplantation mouse development: whole embryo culture and micro-manipulation, Int. J. Dev. Biol. 42 (1998) 895-902.

[17] L. Coultas, K. Chawengsaksophak, J. Rossant, Endothelial cells and VEGF in vascular development, Nature 438 (2005) 937-945.

[18] H. Ohta, K. Sato, N. Murata, et al., Ki16425, a subtype-selective antagonist for EDG-family lysophosphatidic acid receptors, Mol. Pharmacol. 64 (2003) 994-1005.

[19] M.D. Davis, J.J. Clemens, T.L. Macdonald, K.R. Lynch, Sphingosine 1-phosphate analogs as receptor antagonists, J. Biol. Chem. 280 (2005) 9833-9841.

[20] S.W. Nam, T. Clair, Y.S. Kim, A. McMarlin, E. Schiffmann, L.A. Liotta, M.L. Stracke, Autotaxin (NPP-2), a metastasis-enhancing motogen, is an angiogenic factor, Cancer Res. 61 (2001) 6938-6944.

[21] J.S. Karliner, Lysophospholipids and the cardiovascular system, Biochim. Biophys. Acta 1582 (2002) 216-221.

[22] C.M. Rivera-Lopez, A.L. Tucker, K.R. Lynch, Lysophosphatidic acid (LPA) and angiogenesis, Angiogenesis 11 (2008) 301-310.

[23] S.T. Teo, Y.C. Yung, D.R. Herr, J. Chun, Lysophosphatidic acid in vascular development and disease, IUBMB Life 61 (2009) 791-799.

[24] S. Offermanns, V. Mancino, J.P. Revel, M.I. Simon, Vascular system defects and impaired cell chemokinesis as a result of Galpha13 deficiency, Science 275 (1997) 533-536.

[25] J.L. Gu, S. Muller, V. Mancino, S. Offermanns, M.I. Simon, Interaction of G alpha(12) with G alpha(13) and G alpha(q) signaling pathways, Proc Natl Acad Sci U S A 99 (2002) 9352-9357.

[26] J. Yang, M. Boerm, M. McCarty, C. Bucana, I.J. Fidler, Y. Zhuang, B. Su, Mekk3 is essential for early embryonic cardiovascular development, Nat. Genet. 24 (2000) 309-313.

[27] H. J. Liao, T. Kume, C. McKay, M.J. Xu, J.N. Ihle, G. Carpenter, Absence of erythrogenesis and vasculogenesis in Plcg1-deficient mice, J. Biol. Chem. 277 (2002) 9335-9341.

[28] E. Lelievre, P.M. Bourbon, L.J. Duan, R.L. Nussbaum, G.H. Fong, Deficiency in the p110alpha subunit of PI3K results in diminished Tie2 expression and Tie2(-/-)-like vascular defects in mice, Blood 105 (2005) 3935-3938.

[29] J.M. Rogers, G.P. Daston, M.T. Ebron, B. Carver, J.G. Stefanadis, C.T. Grabowski, Studies on the Mechanism of Trypan Blue Teratogenicity in the Rat Developing In Vivo and In Vitro, Teratology 31 (1985) 389-399.

[30] J.B. Lloyd, Cell physiology of the rat visceral yolk sac: a study of pinocytosis and lysosome function, Teratology 41 (1990) 383-393.

[31] W.P. Jollie, Development, morphology, and function of the yolk-sac placenta of laboratory rodents, Teratology 41 (1990) 361-381.

[32] M. Bielinska, N. Narita, D.B. Wilson, Distinct roles for visceral endoderm during embryonic mouse development, Int. J. Dev. Biol. 43 (1999) 183-205.

Figure Legends

Figure 1. Head cavity formation and yolk sac angiogenic defects in *Enpp2*$^{-/-}$ embryos. (A-H) Gross appearance and histological sections. Lateral views (A, C, F-H) and frontal views (D). WT indicates *Enpp2*$^{+/+}$ or *Enpp2*$^{+/-}$ embryos; -/- indicates *Enpp2*$^{-/-}$ embryos. At E7.5, blisters were formed between the embryonic endoderm and mesoderm in *Enpp2*$^{-/-}$ embryos (arrow, A; asterisk, B). At E8.5-E9.5, large cavities were formed in the head mesenchyme (hm) (arrows, C-D, F-G; asterisk, E). At E9.5, the *Enpp2*$^{-/-}$ embryos became much smaller than the controls (F). Some mutant embryos showed cavities in the trunk region (arrowheads) (G). At E9.5, large vitelline vessels were formed in the control (black arrow, H) but not in the *Enpp2*$^{-/-}$ yolk sac. Abbreviations: am, amnion; ch, chorion; ne, neuroepithelium; ys, yolk sac. Scale bars: 480 μm (A, C, D), 280 μm (B), 250 μm (E), and 1.3 mm (F-H). (I-X) Immunostaining of PECAM-1 and smooth muscle actin (SMA). At E8.5, the primary vascular plexus had formed nearly normally in the *Enpp2*$^{-/-}$ yolk sac, although the honeycomb-like patterns were slightly rough and the capillaries slightly dilated (J, L, N). At E9.5, branched vascular networks were seen in the controls (Q), but not in the *Enpp2*$^{-/-}$ yolk sacs (R). Abnormally dilated spaces were formed in the *Enpp2*$^{-/-}$ embryos (asterisks, T, V, X). Abbreviations: ep, embryo proper; epc, epiplacental cone; ve, visceral endoderm. Scale bars: 600 μm (I-J), 220 μm (K-L, S-T), 40 μm (M-N, U-V), 30 μm (O-P, W-X), and 450 μm (Q-R). (Y) RT-PCR of angiogenesis-related genes. RT(-) indicates a control reaction without reverse transcriptase.

Figure 2. Blockade of LPA receptors results in head cavity formation and yolk sac angiogenic defects. (A-L) Gross appearance of the yolk sac and embryo after they were cultured for 1 or 2 days *in vitro* (DIV). (M-P) Vitelline vessels revealed by whole-mount lacZ staining. *Enpp2*$^{-/-}$ embryos showed both head cavity formation (arrow, F) and yolk

sac angiogenic defects (J, N). Arrowheads in (J) indicate the mesodermal cell layers separated from the yolk sac. Mouse embryos cultured with 10 μM Ki16425 (an LPA_1/LPA_3 antagonist) showed head cavity formation (arrow, G), whereas those cultured with 10 μM Ki16425 or 10 μM VPC23019 (an $S1P_1/S1P_3$ antagonist) showed angiogenic defects (K-L, O-P). Scale bar: 600 μm (A-H), 800 μm (I-L), and 250 μm (M-P). (Q-T) Effects of Ki16425 (Ki) and VPC23019 (VPC) on cultured embryos. Data show the percentages of embryos with head cavity formation or yolk sac angiogenic defects. A low concentration (1 μM) of Ki16425, which had a marginal effect on wild-type (+/+) embryos, induced both head cavity formation and angiogenic defects in *Enpp2* heterozygous (+/-) embryos (S-T). The number of embryos examined is shown in each column. The asterisks over the columns represent significant differences (* $P < 0.05$, ** $P < 0.01$, and *** $P < 0.001$) as compared with the wild-type (WT) or control embryos (chi-square test for independence).

Figure 3. Blockade of the Rho/ROCK pathway results in head cavity formation and yolk sac angiogenic defects. (A-L) Gross appearance of the yolk sac and embryo after they were cultured for 1 or 2 days *in vitro* (DIV). (M-R) Vitelline vessels revealed by whole-mount lacZ staining. Mouse embryos cultured in the presence of a Rho inhibitor (20 μg/ml C3 exoenzyme; A, G, M) or a ROCK inhibitor (0.1 μM H1152; B, H, N) showed both head cavity formation and yolk sac angiogenic defects. Mouse embryos cultured with the inhibitors of G_i (0.5 μg/ml pertussis toxin; PTX), phosphatidylinositol 3-kinase (10 μM LY294002), MAP kinase (10 μM PD98059), or phospholipase C (10 μM U-73122) showed angiogenic defects. Scale bar: 60 μm (A-F), 80 μm (G-L), and 25 μm (M-P). (S-T) Percentages of embryos with head cavity formation and yolk sac angiogenic defects

after inhibitor treatment. The number of embryos examined is shown in each column. The asterisks over the columns represent significant differences (*$P < 0.05$, **$P < 0.01$, and ***$P < 0.001$) as compared with the control embryos (chi-square test for independence).

Figure 4. Blockade of actin polymerization results in head cavity formation and yolk sac angiogenic defects. (A-D) Gross appearance of the yolk sac and embryo after they were cultured for 1 or 2 days *in vitro* (DIV). Lateral view (B) and frontal views (A, C-D). (E) Vitelline vessels revealed by whole-mount lacZ staining. Mouse embryos cultured with an actin polymerization inhibitor, cytochalasin B (0.3 μM), showed head cavity formation (arrow, C) and angiogenic defects (E). Scale bar: 600 μm (A-B), 400 μm (C), 800 μm (D), and 250 μm (E). (F-G) Percentages of embryos with head cavity formation and/or yolk sac angiogenic defects after cytochalasin B treatment. The number of embryos examined is shown in each column. The asterisks over the columns represent significant differences (*$P < 0.05$ and **$P < 0.01$) as compared with the control embryos (chi-square test for independence).

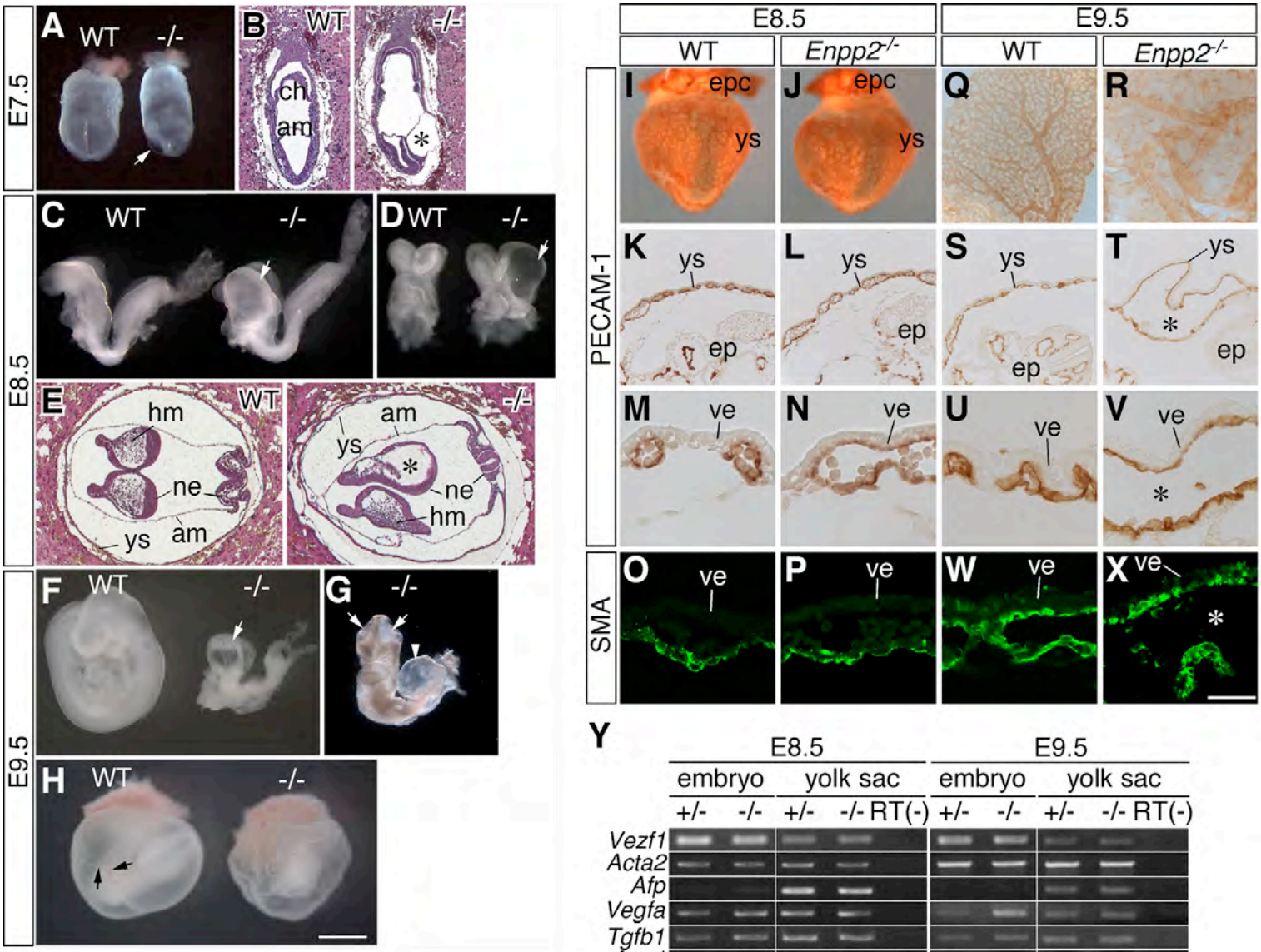

Koike *et al.* Fig. 1

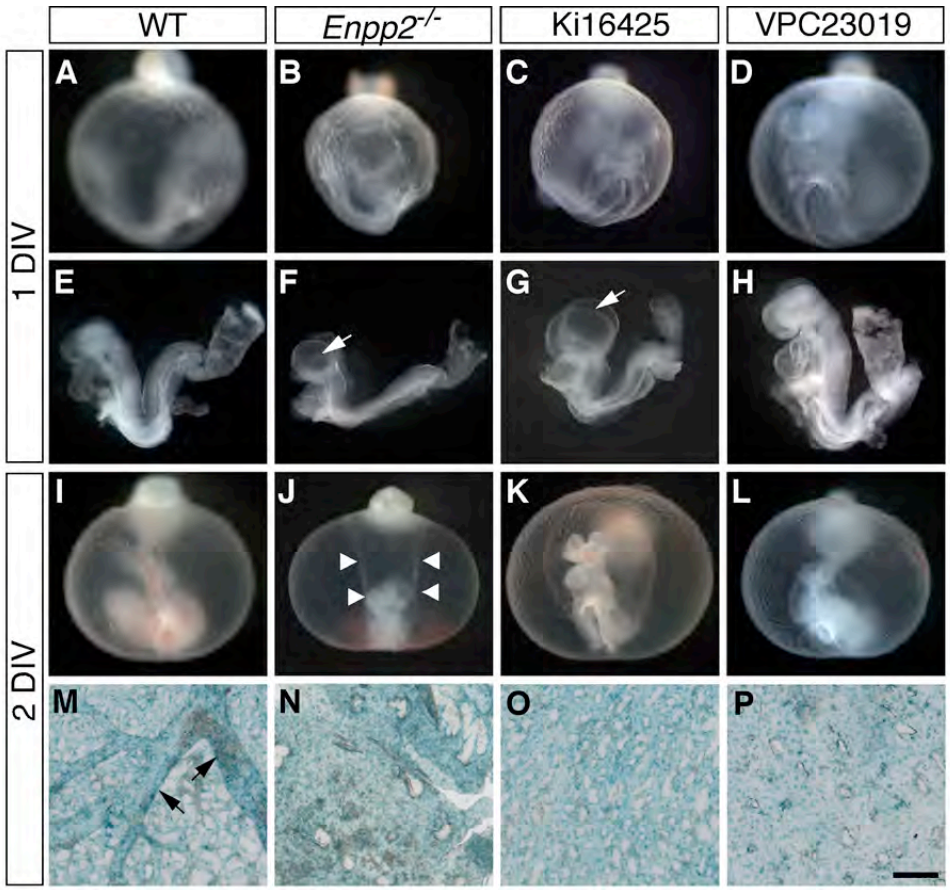

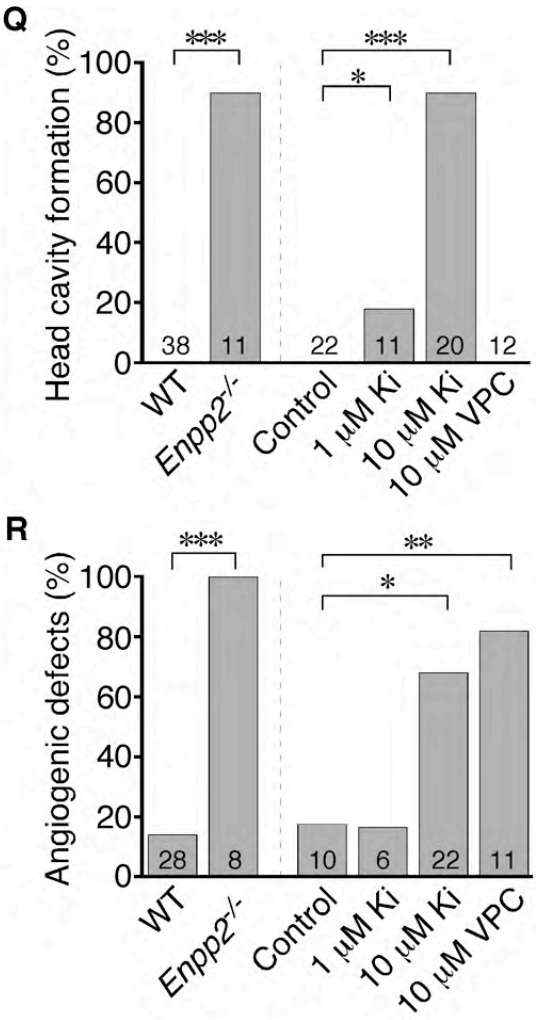

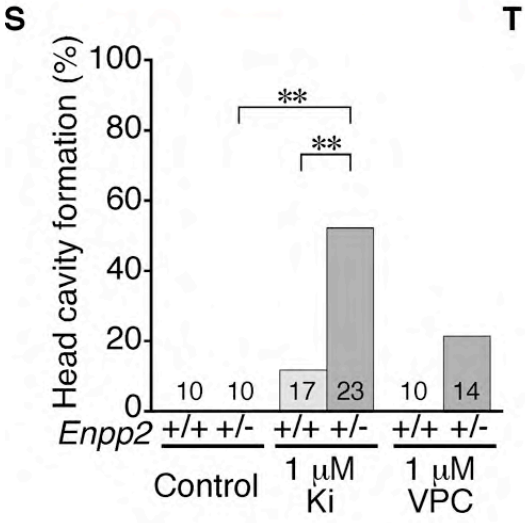

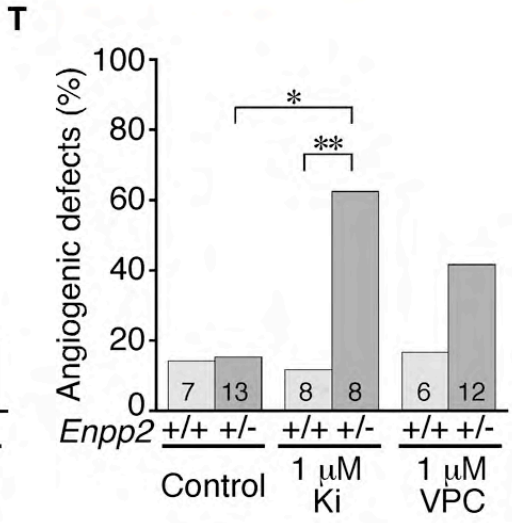

Koike *et al.* Fig. 2

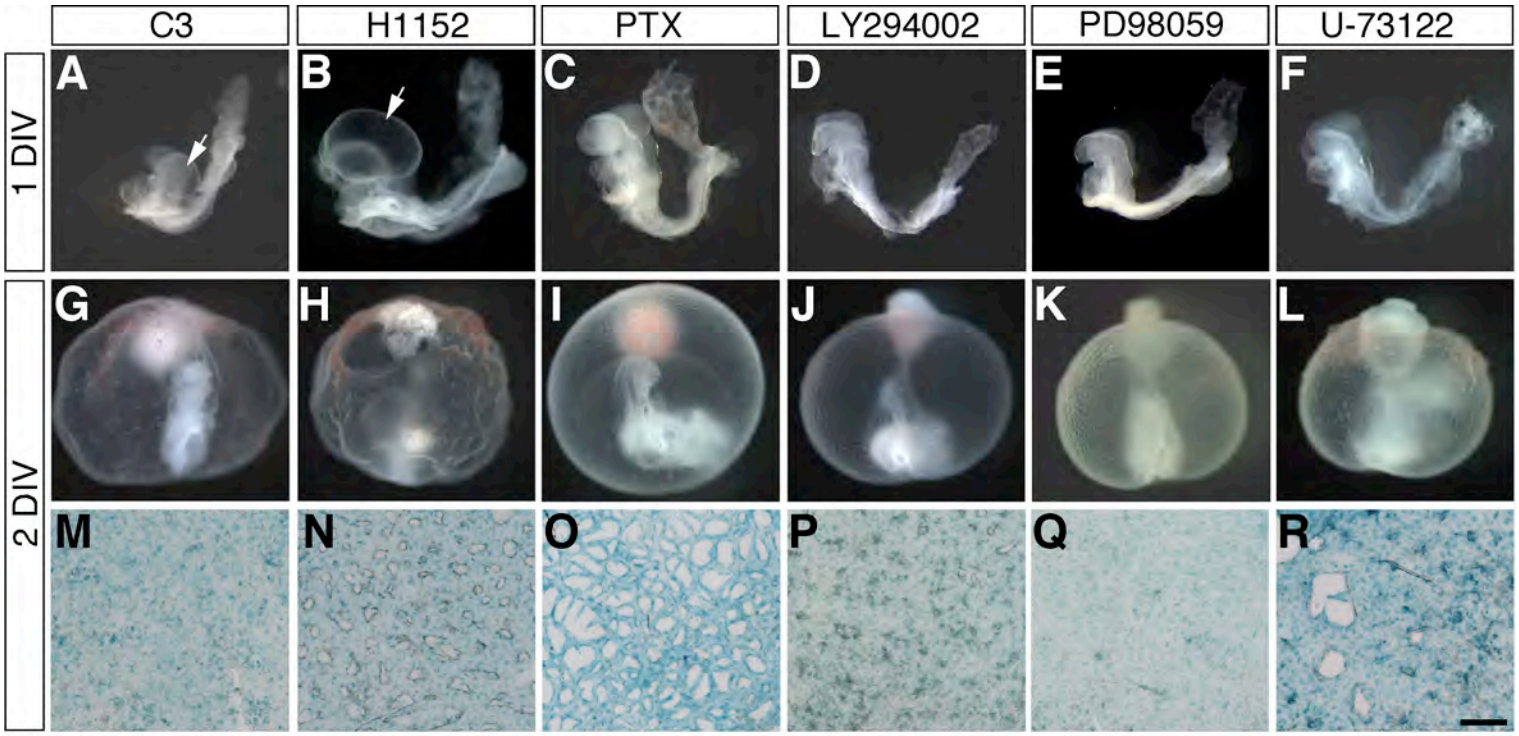

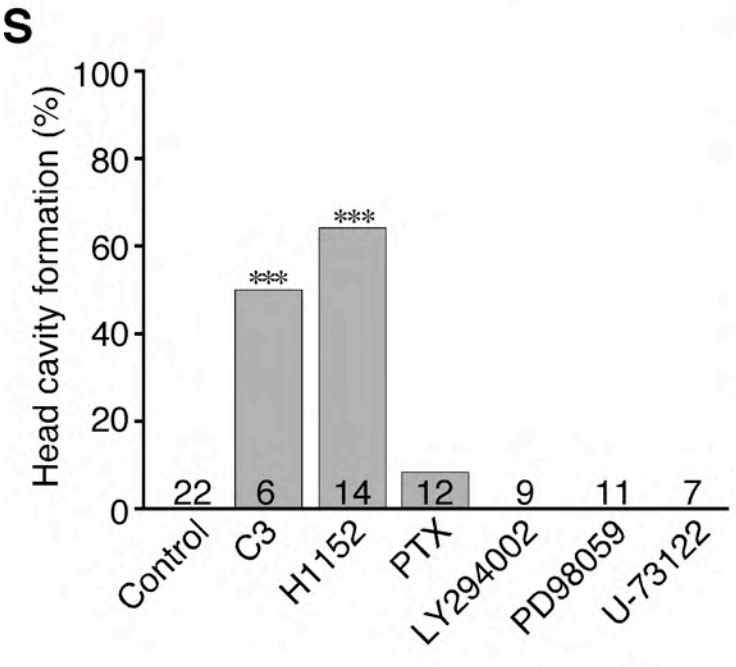

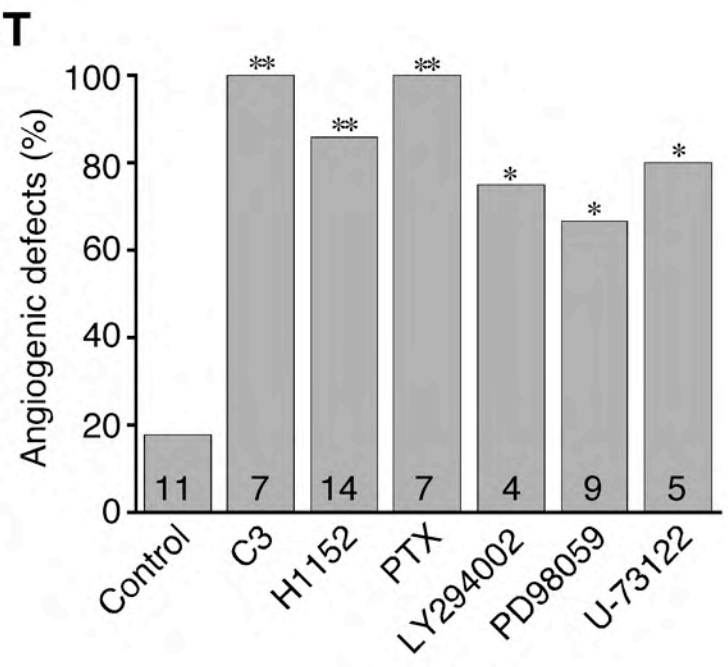

Koike *et al.* Fig. 3

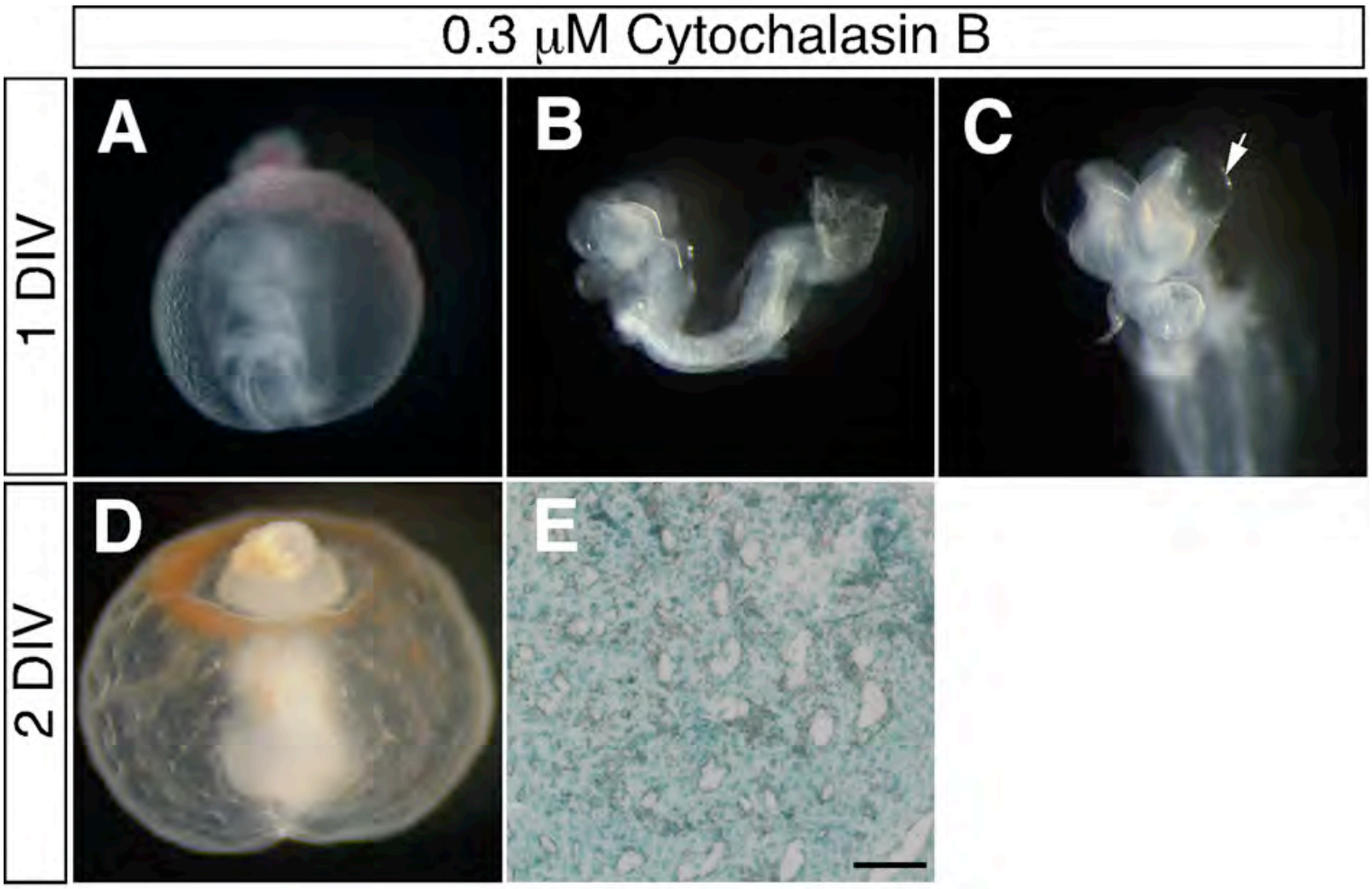

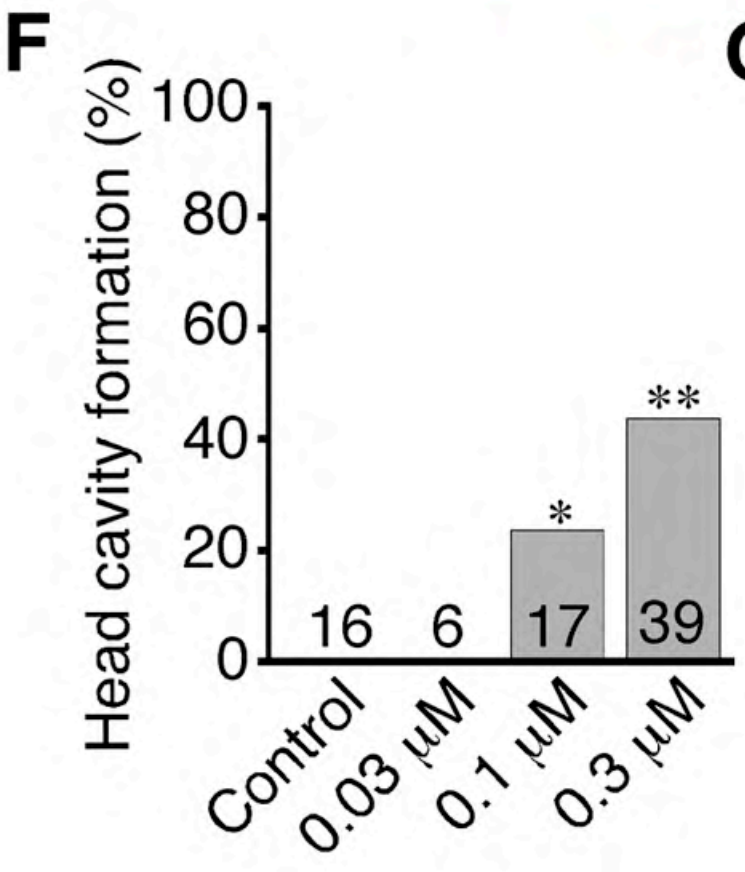

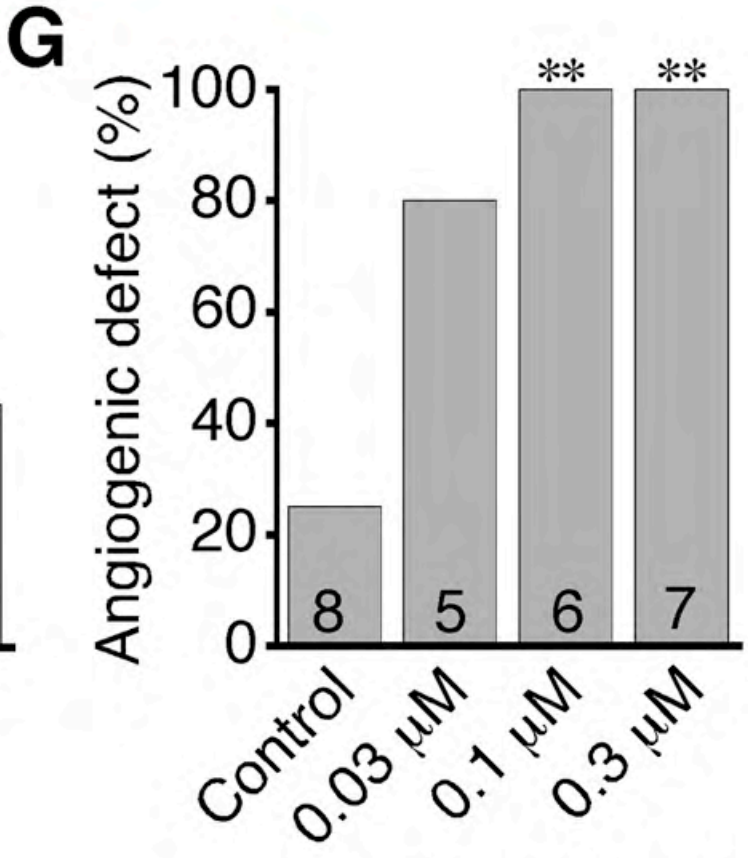

Koike *et al.* Fig. 4